THE JOURNAL OF PHYSICAL CHEMISTRY C

Article

pubs.acs.org/JPCC

# Fractional Diffusion Equation and the Electrical Impedance: Experimental Evidence in Liquid-Crystalline Cells

F. Ciuchi,[†] A. Mazzulla,[†] N. Scaramuzza,[†,‡] E. K. Lenzi,[§] and L. R. Evangelista*[,§]

[†]CNR-IPCF UoS di Cosenza, Licryl Laboratory, and Centro di Eccellenza CEMIF.CAL, Università della Calabria, 87036 Arcavacata di Rende, Italy

[‡]Dipartimento di Fisica, Università della Calabria, 87036 Arcavacata di Rende, Italy

[§]Departamento de Física, Universidade Estadual de Maringá, Avenida Colombo 5790, 87020-900 Maringá, Paraná, Brazil

**ABSTRACT:** The electrical impedance data of different nematic liquid-crystal cells are analyzed in the framework of a model in which the diffusion of mobile ions in the bulk is governed by a fractional diffusion equation of distributed order. The boundary conditions at the electrodes limiting the sample are described by an integro-differential equation governing the kinetic at the interface that embodies, in particular, the usual kinetic equation for describing the adsorption−desorption process at the electrodes but is expressed in terms of a temporal kernel that can be chosen to cover scenarios that are not suitably described within the usual framework of blocking electrodes. The analysis is carried out by supposing that the positive and negative ions have the same mobility and that the electric potential profile across the sample satisfies the Poisson's equation. The results cover a rich variety of scenarios, including the ones connected to anomalous diffusion.

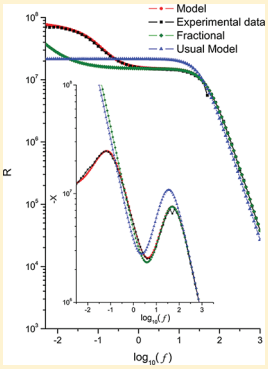


## I. INTRODUCTION

Impedance or immittance spectroscopy is commonly used to analyze electrical response data in the frequency domain of electrolytic cells and, in particular, in liquid-crystalline (LC) cells.[1−5] For understanding the basic properties of LC cells in view of their usefulness in display technology, it is crucial to have knowledge of the mechanisms of transport and accumulation of charges in these systems.[6−9] To face the high complexity of the electrical response of condensed matter systems, we have considered several formalisms, starting with the one that generalizes the Warburg model for the electrical impedance,[1] passing through the treatment of the diffusion of mobile ions by means of fractional calculus in the time domain,[10−13] and arriving, more recently, to models that solve fractional diffusion equations for the mobile ions together with the Poisson's equation for the spatial profile of the electric potential,[14−16] showing that the anomalous diffusion may play an important role in describing the experimental behavior.[17]

In this Article, we analyze impedance spectroscopy data of several LC systems in the framework of a very general physical model recently proposed.[18] In this model, the mathematical problem of a diffusion equation of distributed order[19−21] for the mobile ions coupled to the Poisson's equation for the electrical potential in the bulk but now subjected to boundary conditions that are stated by means of an integro-differential expression is analytically solved.[18] These boundary conditions embody, in particular, the usual kinetic equation for describing the adsorption−desorption process at the electrodes[22] but is expressed in terms of a temporal kernel that can be appropriately chosen to cover scenarios that are not suitably described within the usual framework of blocking electrodes.

## II. EXPERIMENTAL SECTION

Two classes of samples having different kind of electrodes, 1 × 1 $cm^2$ surface area, on transparent glass plates were prepared. The first electrode consists of an evaporated gold pixel whose thickness is 30 nm; the second one is made of indium tin oxide (ITO). Alignment of liquid crystal was achieved by rubbing thin polyimide layers spin-coated onto the electrodes. Different values of polyimide thicknesses have been used, that is, 5, 20, and 50 nm, obtained by spin-coating the glasses with 2, 10, and 20 wt % solutions of LQ1800 (Hitachi) in methyl pyrrolidinone, respectively. The cells were obtained by assembling two slides, prepared as described above and placed parallel to each other, using Mylar spacers between them of 30 $\mu$m nominal thickness.

The complex impedance has been measured by a potentiostat/galvanostat/impedentiometer EG&G model 273A in a frequency range from $10^{-3}$ to $10^{5}$ Hz. Low amplitude of the sinusoidal applied voltage was chosen, 25 mV pp, to avoid electrically induced reorientation of the liquid crystal. One connector acts as working electrode, whereas the counter electrode has been short-circuited with the reference one. Measurements at lower voltages give the same results but introduce more noise. In any case, at the values of the applied voltage, no electrochemical effect can be activated in nematic liquid crystals, both in the bulk or due to the electrodes of confinement. Moreover, the polyimide aligning layers prevent

**Received:** November 17, 2011
**Revised:** March 26, 2012
**Published:** April 2, 2012

direct contact between the evaporated gold electrode and the nematic liquid crystals.

## III. FRACTIONAL DIFFUSION MODEL

The first of the fundamental equations of the model is the fractional diffusion equation for the bulk density of ions $n_\alpha$ ($\alpha = p$ for positive and $\alpha = n$ for negative ones)

$$\int_0^\infty d\gamma\, \tau(\gamma)\frac{\partial^\gamma}{\partial t^\gamma} n_\alpha(z, t) = -\frac{\partial}{\partial z} j_\alpha(z, t) \tag{1}$$

where $\tau(\gamma)$ is a distribution function of $\gamma$, with the current density given by

$$j_\alpha(z, t) = -D\frac{\partial}{\partial z} n_\alpha(z, t) \mp \frac{qD}{k_B T} n_\alpha(z, t)\frac{\partial V}{\partial z} \tag{2}$$

In eq 2, $D$ is the diffusion coefficient for the mobile ions (the same for positive and negative ones) of charge $q$, $V$ is the actual electric potential across a sample of thickness $d$, with the electrodes placed at the positions $z = \pm d/2$, of a Cartesian reference frame in which $z$ is the axis normal to them, $k_B$ is the Boltzmann constant, and $T$ is the absolute temperature. The choice of $\gamma \neq 1$ permits us to consider a richer scenario in which different diffusive regimes (i.e., different values of $\gamma$) may occur depending on the distribution $\tau(\gamma)$ for the fractional time derivative of distributed order. The presence of these regimes is expected to play an important role in reproducing the experimental data regarding the real part of the impedance because in the low-frequency limit they introduce a different behavior for the impedance, as pointed out in ref 14. Indeed, the experimental data shown in Figures 1 and 2 present a frequency behavior similar to the one shown in figure 3 of ref 14 that can be interpreted as indicating the presence of at least two different diffusive regimes, that is, one of them manifested in the low-frequency region and another one in the high-frequency limit. Similar features can also be verified in others systems such as the ones worked out in ref 15. The imaginary part of the impedance also exhibits at low frequency an anomalous behavior that may be described by considering eq 1 subjected to the boundary conditions

$$j_\alpha(z, t)|_{z=\pm d/2} = \pm\int_{-\infty}^{t} d\bar{t}\; \kappa(t - \bar{t})\frac{\partial^\eta}{\partial \bar{t}^\eta} n_\alpha(z, \bar{t})\Big|_{z=\pm d/2} \tag{3}$$

Notice that the boundary condition contains a fractional operator[23] that, depending on the sign of $\eta$, may represent a fractional time derivative (if $\eta > 0$) or a fractional integral (if $\eta < 0$). For $0 < \eta \leq 1$, the term on the right side can be related to an adsorption−desorption process. Indeed, for the specific choice of $\kappa(t) = \kappa e^{-t/\tau}$ with $\eta = 1$, we recover the adsorption−desorption processes at the surfaces governed by a kinetic equation that corresponds to the Langmuir approximation.[22] Others choices of $\kappa(t)$ and $\eta$ can be performed to incorporate memory effects and, consequently, non-Debye relaxation processes[24] to cover scenarios where different regimes may also be manifested as one presented in ref 25. In an additional sense, it is also necessary to mention that eq 3 embodies, as a particular case, the Chang−Jaffé boundary conditions[4,5] and, consequently, can be related to the situation characterized by ohmic electrodes.[26] The potential is determined by the Poisson's equation

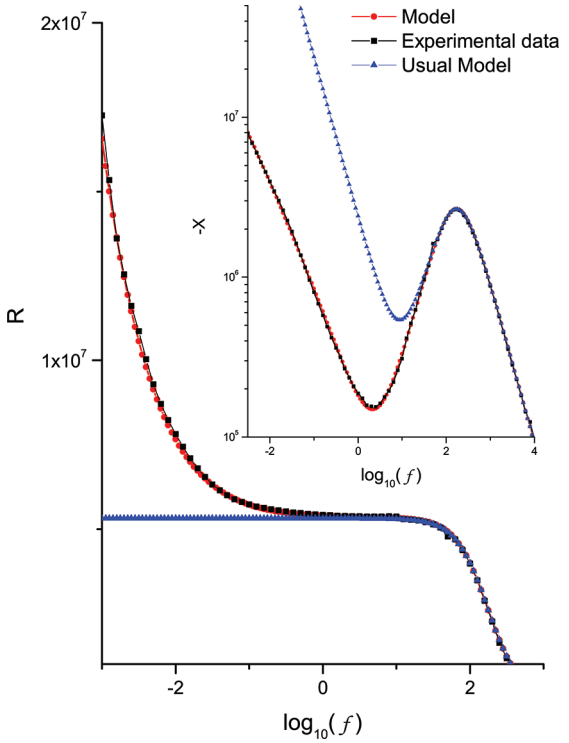


**Figure 1.** Real ($R$) and imaginary ($X$) parts of the electrical impedance of the cell versus the frequency of the applied voltage, $f = \omega/2\pi$. The Figure was drawn for parameters (in SI units): $\mathcal{S} = 10^{-4}$, $d = 36 \times 10^{-6}$, $\varepsilon = 7\varepsilon_0$, $\mathcal{D} = 4.7 \times 10^{-12}$, $\kappa = 7.5 \times 10^{-7}$, $\tau = 1.6$, $\lambda = 6.574 \times 10^{-8}$, $\vartheta_1 = 0.45$, $\vartheta_2 = \vartheta_1/4$, $\kappa_1 = \kappa$, $\eta = 1$, and $\gamma = 1$ ($A = 1$). Note that the results predicted by the model described in the previous section correspond to the red line, and the usual model,[22] characterized by a blue line, is obtained from eq 5, with $\kappa = 0$ and $\gamma = 1$. The experimental data, represented by the black line, correspond to the sample AU2. (See the text.)

$$\frac{\partial^2}{\partial z^2} V(z, t) = -\frac{q}{\varepsilon}[n_+(z, t) - n_-(z, t)] \tag{4}$$

which depends on the difference between the densities of charged particles. These equations govern the dynamics of the system and have been analytically solved,[18] giving the impedance of the cell in the form

$$\mathcal{Z} = \frac{2}{i\omega\varepsilon\mathcal{S}\beta^2} \times \frac{\tanh(\beta d/2)/(\lambda^2\beta) + d\mathcal{E}/(2\mathcal{D})}{1 + (i\omega)^{\eta-1}\kappa(i\omega)(1 + i\omega\lambda^2/D)\tanh(\beta d/2)/(\lambda^2\beta)} \tag{5}$$

where $S$ is the electrode area and $\lambda = (\varepsilon k_B T/(2Nq^2))^{1/2}$ is the Debye's screening length. In eq 5, the other quantities are

$$\beta = \sqrt{\frac{F(i\omega)}{D} + \frac{1}{\lambda^2}} \quad \text{with} \quad F(i\omega) = \int_0^\infty d\gamma\, \tau(\gamma)(i\omega)^\gamma \tag{6}$$

and $\mathcal{E} = F(i\omega) + \beta(i\omega)^\eta\kappa(i\omega)\tanh(\beta\, d/2)$, in which the transformed kernel is given by

$$\kappa(i\omega) = e^{-i\omega t}\int_0^\infty dt'\, k(t - t')e^{i\omega t'} \tag{7}$$

The presence of the kernel $k(t - t')$ and of the fractional time derivative on the boundary condition give to the electrical impedance (eq 5) a very general profile. As a matter of fact, for


dx.doi.org/10.1021/jp211097m | J. Phys. Chem. C 2012, 116, 8773−8777

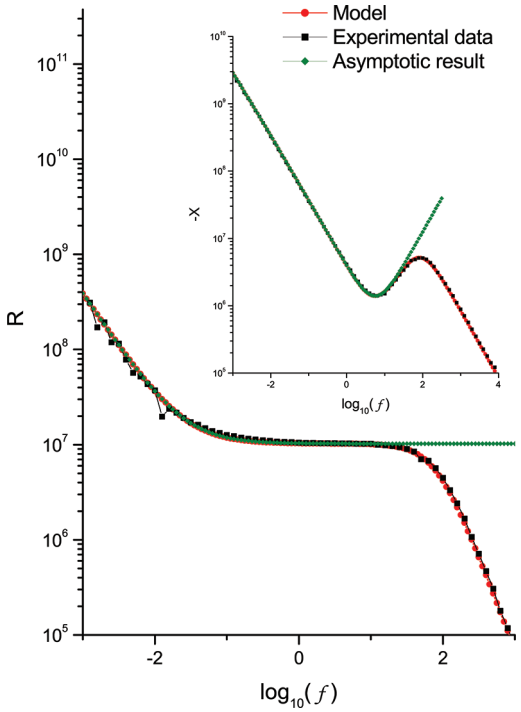


**Figure 2.** Real ($R$) and imaginary ($X$) parts of the electrical impedance of the cell versus the frequency of the applied voltage, $f = \omega/2\pi$. The parameters (in SI units) are $\mathcal{S} = 10^{-4}$, $d = 37 \times 10^{-6}$, $\varepsilon = 7.8\varepsilon_0$, $\mathcal{D} = 4 \times 10^{-12}$, $\kappa = 1.2 \times 10^{-6}$, $\tau = 10^{-3}$, $\lambda = 8.778 \times 10^{-8}$, $\vartheta_1 = 0.285$, $\kappa_1 = 0$, $\eta = 1$, and $\gamma = 1$ ($A = 1$). The experimental data illustrated by the black line correspond to the sample ITO10, and the green line represents the results obtained from eq 8. Similarly to what happens in Figure 1, the red line is obtained by means of eq 5 with the previous values for the parameters.

$\tau(\gamma) = \delta(\gamma - 1)$, $\eta = 1$, with $k(t) = \kappa e^{-t/\tau}$, the case worked out in ref 22, in which adsorption−desorption phenomena are incorporated into the analysis by means of a kinetic balance equation at the surfaces, is recovered. Moreover, for $\tau(\gamma) = \delta(\gamma - 1)$, with $k(t) = 0$, the usual form of the electrical impedance obtained in the situation of blocking electrodes is reobtained.

The asymptotic behavior for eq 5 in the low-frequency limit depends on the choice of $F(i\omega)$ and $\kappa(i\omega)$. To investigate this behavior in detail we consider that $F(i\omega) \approx (i\omega)^{\delta}$ $(0 < \delta \leq 1)$ and $\kappa(i\omega) \approx 1/(i\omega)^{\nu}$ $(0 < \nu < 1)$, when $\omega \to 0$. This particular choice for $F(i\omega)$ and $\kappa(i\omega)$ will be employed in the next section to analyze the experimental data. By taking these conditions into account, we obtain the approximated result

$$\mathcal{Z} \approx \frac{\lambda}{i\omega\varepsilon\mathcal{S}} \frac{2 + \lambda(d - \lambda)F(i\omega)/D + (i\omega)^{\eta} d\kappa(i\omega)/D}{1 + (i\omega)^{\eta-1}\kappa(i\omega)/\lambda} \tag{8}$$

in the limit $\omega \to 0$.

## IV. RESULTS AND DISCUSSION

We have analyzed the experimental data by using the approach summarized in the previous section.[18] We have focused our attention on three representative samples, whose frequency behavior of $Z$ was found unusual, deserving a more powerful tool to be explained. The first sample was made by ITO electrodes, corresponding to a spin coating of 10 wt % solution of LQ1800 (ITO10) and two samples of gold electrodes, corresponding to 2 and 20 wt % solution of LQ1800 (respectively, designed hereafter as AU2 and AU20), whose preparation was described before. As a starting point, we have considered the possibility of two different regimes for the diffusion of ions through the sample to reproduce the behavior of the experimental data which, in the low frequency limit, have a frequency dependence on the impedance, in contrast with the usual case, which is verified in the high-frequency limit. This procedure was suggested by the presence of the polymide layers coated onto the electrodes, which are in contact with the insulating medium of interest. To mathematically account for two diffusive regimes, one of them being the usual and another the anomalous one, characterized by a fractional coefficient $\gamma$, it is convenient to choose, for instance, $F(i\omega) = A(i\omega)+(1 - A)(i\omega)^{\gamma}$, where $A$ is a controlling parameter, $0 \leq A \leq 1$, such that $A = 1$ corresponds to a pure usual diffusion ($\gamma = 1$) whereas $A = 0$ to a pure fractional, anomalous, regime ($\gamma \neq 1$). This kind of superposition is suitable because the experimental data obtained for the real part of impedance exhibit a plateau at high frequency and a power-law behavior at low frequency, and, in a phenomenological perspective, it represents some kind of mixing or interpolation of different behaviors for different ranges of frequency. Indeed, the plateau may be connected to an usual diffusive process and the power-law behavior to an anomalous one. Notice, however, that the presence of fractional derivatives in the diffusion equation does not change the asymptotic behavior of the imaginary part of the impedance at low frequency, as discussed in refs 18 and 19. In this regard, the surface effects represented by the boundary conditions, that is, eq 3, play a prominent role and deserve a more detailed analysis. The behavior of the imaginary part of the impedance is influenced by the boundary conditions and, depending on the choice performed for them, different trends can be obtained, as performed in ref 18. In addition, this unusual behavior of the imaginary part may also be connected to an anomalous diffusion process. In fact, surfaces effects may induce anomalous diffusion, as show in ref 25. To investigate these surface effects in more detail, we have considered $\kappa(i\omega) = \kappa\tau(1/(i\omega\tau)^{\vartheta_1} + (\kappa_1/\kappa)/(i\omega\tau)^{\vartheta_2})$. This choice for $\kappa(i\omega)$, made to perform a phenomenological description of the surface effect on the ions, considers the presence of two processes occurring at the electrodes with a characteristic time, $\tau$. Of these processes, one is delocalized along a characteristic surface thickness, $\kappa\tau$, and another one along the thickness $\kappa_1\tau$. Consequently, the parameters $\vartheta_1$, $\vartheta_2$ are connected to effects produced by the surfaces, and $\gamma$ is connected to effects produced by the bulk on the dynamics of the mobile ions.

In Figure 1, the frequency dependence of the real ($R$) and imaginary ($X$) parts of the electrical impedance are shown for the sample AU2 for the case in which the ion diffusion in the bulk was treated as usual, that is, for $\gamma = 1$. The kernel corresponding to the surface part was such that the characteristic surface lengths were $\kappa\tau = \kappa_1\tau = 1.2$ $\mu$m. These lengths have to be compared with the thickness of the sample, $d = 36$ $\mu$m, and the Debye's screening length, $\lambda \approx 0.065$ $\mu$m. For this sample, the surface effects are very pronounced and delocalized along a mesoscopic length corresponding to >3% of the thickness of the sample. For comparative purposes, in the same Figure is shown the usual behavior, that is, the usual diffusion equation for the diffusion of bulk ions together with the blocking electrodes boundary condition. This usual solution is characterized by a plateau in the low-frequency region, which is absent in the experimental data. Therefore, to explain the low-frequency dependence of the electrical impedance, we have


dx.doi.org/10.1021/jp211097m | J. Phys. Chem. C 2012, 116, 8773−8777

used a simple kernel in which two different power law behaviors intervene in the form $\kappa(i\omega)/\kappa\tau \approx 1/(i\omega\tau)^{0.45}+1/(i\omega\tau)^{0.11}$.

The same quantities are exhibited for the sample ITO10 in Figure 2. For this sample, there is only one characteristic surface length, namely, $\kappa\tau = 1.2 \times 10^{-3}$ $\mu$m ($\kappa_1\tau = 0$) to be compared with the thickness of the sample, $d = 37$ $\mu$m, and the Debye's screening length, $\lambda = 87.78 \times 10^{-3}$ $\mu$m. We observe that the surface effects are still delocalized and are also important in determining the anomalous behavior of the impedance. The low-frequency behavior is essentially governed by a kernel (surface) having the form $\kappa(i\omega)/\kappa\tau \approx 1/(i\omega\tau)^{0.285}$, but the diffusion of ions in the bulk is the normal one, that is, $\gamma = 1$.

A still more complex behavior was found in the AU20 sample, shown in Figure 3. Now, the best agreement was

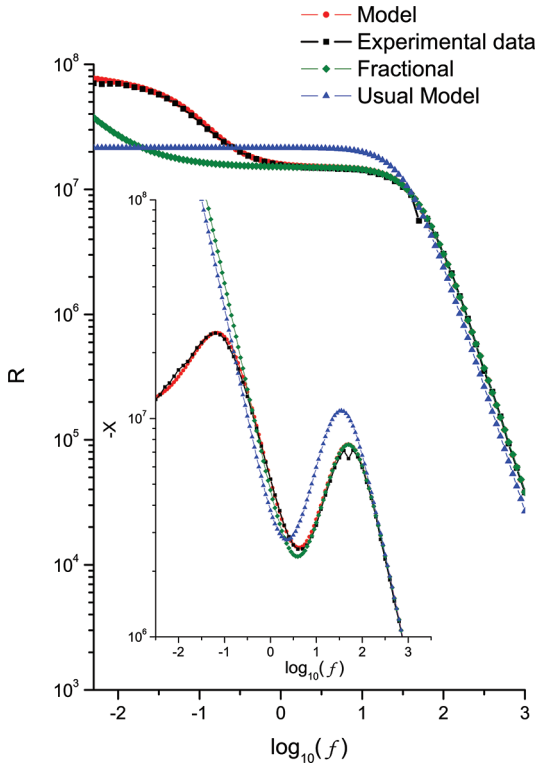


**Figure 3.** Real ($R$) and imaginary ($X$) parts of the electrical impedance of the cell versus the frequency of the applied voltage, $f = \omega/2\pi$. The parameters (in SI units) are $\mathcal{S} = 10^{-4}$, $d = 36 \times 10^{-6}$, $\varepsilon = 8.5\varepsilon_0$, $\mathcal{D} = 1.05 \times 10^{-12}$, $\kappa = 1.1 \times 10^{-7}$, $\tau = \times 10^{-2}$, $\lambda = 1.0337 \times 10^{-7}$, $\vartheta_1 = 0.864$, $\vartheta_2 = 0.2$ $\kappa_1 = \kappa$, $\eta = 1$, and $\gamma = 0.16$. The experimental data correspond to the sample AU20. The red line corresponds to results obtained from eq 5 with the previous values for the parameters. The fractional[14] and usual[22] models are obtained from eq 5 by considering $\kappa = 0$ with $\gamma \neq 1$ and $\kappa = 0$ with $\gamma = 1$.

obtained by invoking the anomalous process for the bulk, governed by a fractional diffusion equation with $\gamma = 0.16$, and a largely delocalized surface influence, characterized by the length $\kappa\tau = \kappa_1\tau \approx 10^{-3}\mu$m, whereas the thickness of the sample is $d = 36$ $\mu$m and the Debye's screening length is $\lambda \approx 0.10337$ $\mu$m.

Finally, in Figure 4, the imaginary ($X$) versus the real part ($R$) of the impedance is shown for the systems presented in Figures 1−3.

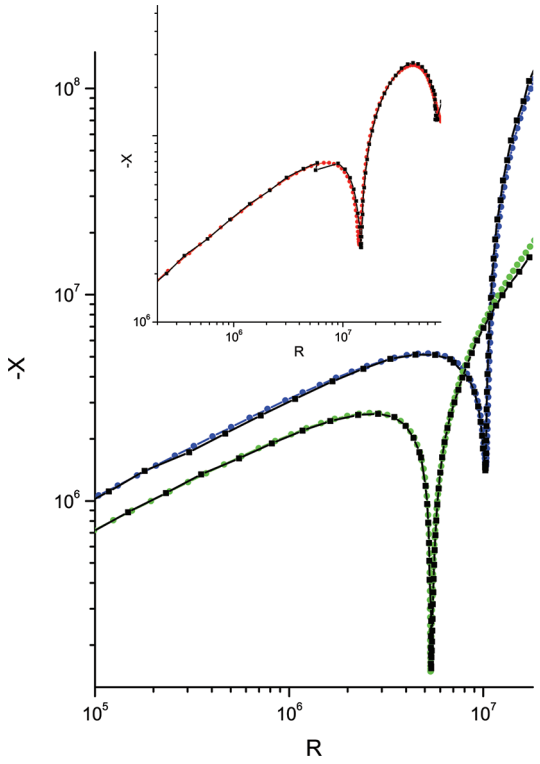


**Figure 4.** Imaginary part of the impedance versus the real part of the impedance for the samples we are analyzing: AU2 (bottom), ITO10 (middle), and AU20 (top). The black line corresponds to the experimental data, and the red, blue, and green lines represent eq 5 with the parameters values used in Figures 1−3.

## V. CONCLUSIONS

We have investigated the electrical response of an electrolytic cell by considering the diffusion of the ions governed by a fractional equation of distributed order subjected to a boundary condition expressed as an integro-differential equation. The fractional diffusion equation of distributed order is connected to anomalous diffusion and recovers the usual diffusion in the appropriated limit. It can also be used to investigate situations in which different diffusive regimes are present. The boundary conditions considered here extend the ones usually employed to investigate these systems and can lead us to situations connected to anomalous diffusion. The values of the parameters in agreement with the experimental data have shown that the imaginary part of the impedance is more influenced by the surface (i.e., the boundary conditions) at low frequency and by the bulk at high frequency. In this respect, it is worth mentioning that in the low-frequency limit the behavior of the real part of the impedance is more influenced by the bulk equation (diffusion equation) than the imaginary part of the impedance is. Anyway, the surface conditions also play an important role in the behavior of the real part of the impedance. Therefore, these results provide evidence that the diffusion process of the ions in these electrolytic cells is anomalous and the mechanisms of these processes may be connected to the surface effects that induce an anomalous process on the bulk.

## AUTHOR INFORMATION

### Corresponding Author

*E-mail: lre@dfi.uem.br. Fax:+55 44 3263 4623. Phone: +55 44 3011 5979.

### Notes

The authors declare no competing financial interest.

## ■ ACKNOWLEDGMENTS

This work was partially supported by the National Institutes of Science and Technology (INCT-CNPq) of Complex Systems (E.K.L.) and Complex Fluids (L.R.E.). We thank Alfredo Pane for the samples preparation in clean room.

## ■ REFERENCES

(1) Macdonald, J. R. *J. Appl. Phys.* **1985**, *58*, 1955−1970.
(2) Johnson, W. B.; Macdonald, J. R. Fundamental of Impedance Spectroscopy. In *Impedance Spectroscopy, Theory, Experiment, and Applications*; Barsoukov, E., Macdonald, J. R., Eds.; Wiley: New York, 2005; pp 1−26.
(3) Raistrick, I. D.; Franceschetti, D. R.; Macdonald, J. R. Theory. In *Impedance Spectroscopy, Theory, Experiment, and Applications*; Barsoukov, E., Macdonald, J. R., Eds.; Wiley: New York, 2005; pp 27−128.
(4) Macdonald, J. R. *J. Electroanal. Chem.* **1976**, *70*, 17−26.
(5) Macdonald, J. R.; Franceschetti, D. R. *J. Chem. Phys.* **1978**, *68*, 1614−1637.
(6) Murakami, S.; Naito, H. *Jpn. J. Appl. Phys., Part 1* **1997**, *36*, 2222−2225.
(7) Murakami, S.; Iga, H.; Naito, H. *J. Appl. Phys.* **1996**, *80*, 6396−6400.
(8) Verschueren, A. R. M.; Niessen, R. A. H.; Notten, P. H. L.; Oepts, W.; Alexander-Moonen, E. M. L. *IEEE Trans. Dielectr. Electr. Insul.* **2003**, *10*, 963−969.
(9) Barbero, G. *Phys. Rev. E* **2005**, *71*, 062201.
(10) Bisquert, J.; Compte, A. *J. Electroanal. Chem.* **2001**, *499*, 112−120.
(11) Bisquert, J.; Garcia-Belmonte, G.; Pitarch, A. *ChemPhysChem* **2003**, *4*, 287−292.
(12) Bisquert, J. *Phys. Rev. E* **2005**, *72*, 011109.
(13) Bisquert, J. *Phys. Rev. Lett.* **2003**, *91*, 010602.
(14) Lenzi, E. K.; Evangelista, L. R.; Barbero, G. *J. Phys. Chem. B* **2009**, *113*, 11371−11374.
(15) Sidebottom, D. L. *Rev. Mod. Phys.* **2009**, *81*, 999−1014.
(16) Macdonald, J. R. *J. Phys.: Condensed Matter* **2010**, *22*, 495101.
(17) Macdonald, J. R.; Evangelista, L. R.; Lenzi, E. K.; Barbero, G. *J. Phys. Chem. C* **2011**, *115*, 7648−7655.
(18) Santoro, P. A.; de Paula, J. L.; Lenzi, E. K.; Evangelista, L. R. *J. Chem. Phys.* **2011**, *135*, 114704.
(19) Evangelista, L. R.; Lenzi, E. K.; Barbero, G.; Macdonald, J. R. *J. Phys.: Condens. Matter* **2011**, *23*, 485005.
(20) Chechkin, A. V.; Gonchar, V. Yu.; Gorenflo, R.; Korabel, N.; Sokolov, I. M. *Phys. Rev. E* **2008**, *78*, 021111.
(21) Lenzi, E. K.; Mendes, R. S.; Tsallis, C. *Phys. Rev. E* **2003**, *67*, 031104.
(22) Barbero, G.; Evangelista, L. R. *Adsorption Phenomena and Anchoring Energy in Nematic Liquid Crystals*; Taylor & Francis: London, 2006.
(23) Podlubny, I., *Fractional Differential Equations*; Academic Press: San Diego, 1999.
(24) Lenzi, E. K.; Yednak, C. A. R.; Evangelista, L. R. *Phys. Rev. E* **2010**, *81*, 011116.
(25) Lenzi, E. K.; Evangelista, L. R.; Barbero, G.; Mantegazza, F. *Europhys. Lett.* **2009**, *85*, 28004.
(26) Batalioto, F.; Barbero, G.; Figueiredo Neto, A. M. *J. Appl. Phys.* **2007**, *102*, 104111.